Utah State University
DigitalCommons@USU

Senior Theses and Projects | Materials Physics

5-9-2014

Improved Measurements in Conductivity for Highly Disorganized Resistive Materials

Phil Lundgreen
Utah State University

Follow this and additional works at: https://digitalcommons.usu.edu/mp_seniorthesesprojects

Part of the Condensed Matter Physics Commons

Recommended Citation

Improved Measurements in Conductivity for Highly Disorganized Resistive Materials Phil Lundgreen Department of Physics 4900 Project Research Mentor: J.R. Dennison April 22, 2014

This Report is brought to you for free and open access by the Materials Physics at DigitalCommons@USU. It has been accepted for inclusion in Senior Theses and Projects by an authorized administrator of DigitalCommons@USU. For more information, please contact digitalcommons@usu.edu.

Improved Measurements in Conductivity for Highly Disorganized Resistive Materials

Phil Lundgreen

Department of Physics
4900 Project
Research Mentor: J.R. Dennison
April 22, 2014

Introduction

Determining the electrical properties of highly insulating materials can be a challenging task. These materials are designed to greatly resist the flow of electrical current. This makes them useful for various applications including terrestrial transmission lines, spacecraft charging, and capacitor-driven charge storage devices. Every year over 370 billion kWhr are lost during transportation along power lines in the US. That is roughly $36B which is thrown away each year due to inefficiency in our power transmission network (1). Due to the fact that satellites are isolated from ground, charging caused by the plasma environment found at typical orbital radii (2) is of concern to the designers of modern spacecraft (3).

In an effort to measure extremely low currents and low conductivity, the Utah State University Materials Physics Group has designed a Constant Voltage Chamber (CVC) capable of measuring conductivity with a low degree of uncertainty. Over the last nine years, many changes have been made to improve the accuracy and precision of measurements made with the CVC, now allowing currents as low as hundreds of atto-amps to be measured (3, 4, 5,6). Through the use of a variety of data analysis programs, numerous studies of the conductivity, current, and temperature have been done with detailed error analysis. Statistical analysis has been performed for the data collected and the instrumentation error for the system has been determined (7). These data have allowed for analysis of the different aspects of current, and allowed for better measurements to be made. Using these measurements we have been able to create a model for the rate of change for the different aspects of current involved with a highly resistive material.

How Charge Propagates

Charge propagating through an insulating media is most simply modeled as a uniform square wave front advancing across the material. A diagram of charge propagation of this nature would appear like (Fig. 1(a)), with a zero-current baseline; once a potential is applied, a straight uniform wall of charge crossing the dielectric at a uniform rate.

This is a good initial model but, in reality, charge propagation behaves more like (Fig. 1(b)). Once a potential is applied to one side of the dielectric, effects from polarization, diffusion, and dispersion disperse the leading edge of charge. (Fig. 2) Thus, charge propagation behavior does not look like a square wave, but rather more like a gradual curve. At different moments, as the dielectric is charging, different aspects of the current will become dominant. This is manifest by temporal changes in the conductivity curve slope,

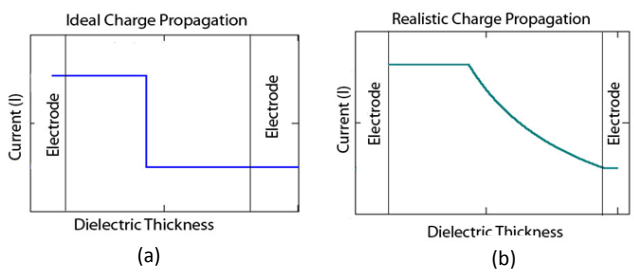

Figure 1. (a) An idealization of charge moving from one electrode where a potential is applied to the other electrode. (b) A more realistic visualization, showing that individual charge carriers propagate at different rates through a dielectric material.

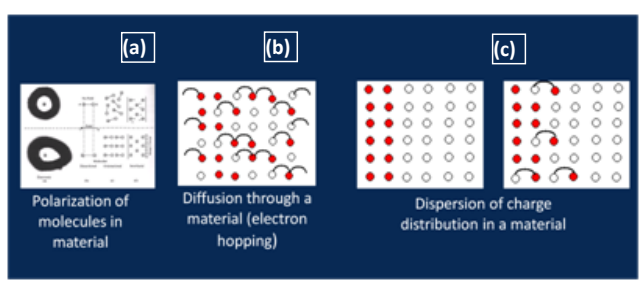

Figure 2. (a) Potential applied to one side of a material will begin to polarize the molecules. (b) The leading edge of charge diffuses across the material. (c) Charge slowly disperses through the material in a wall of charge.

as will be shown in the data analysis of this paper.

Conductivity Measurements

The Constant Voltage Chamber is a unique apparatus designed to take measurements of the conductivity of various insulating materials. To decrease the error associated with data measurements the CVC utilizes a high vacuum pumping system to decrease the pressure within the chamber to 10 orders of magnitude below atmospheric pressure. (8)

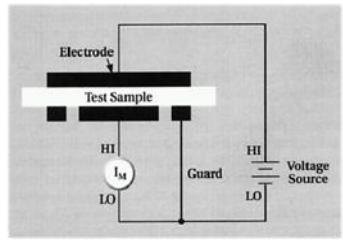

Figure 3 a parallel plate capacitor system

The goal when analyzing insulating materials using the CVC is to determine the conductivity of the material. To do this, a parallel plate capacitor setup has been utilized within the CVC chamber (Fig. 3). Potentials of varying voltages were then applied to the front electrode of the sample, and the current was measured as a function of time from the back electrode (Fig. 3). Conductivity is defined by measurements of the applied voltage (V), current (I), sample thickness (d), and area as(A):

$$\sigma = \frac{I \cdot d}{A \cdot V} \qquad [1]$$

The errors in current, thickness, area, and voltage are added in quadrature to determine the error in conductivity:

$$\frac{\Delta\sigma}{\sigma} = \sqrt{\left(\frac{\Delta I}{I}\right)^2 + \left(\frac{\Delta V}{V}\right)^2 + \left(\frac{\Delta A}{A}\right)^2 + \left(\frac{\Delta d}{d}\right)^2} \qquad [2]$$

Because the area and thickness of samples remain constant, independent of the voltage applied, they contribute only to the absolute uncertainty. For highly resistive materials at low voltages, the error associated with current measurements is much greater than that associated with the voltage (8). To determine the statistical error associated with conductivity, therefore, we should focus on the error associated with the current measurements.

The current as it is measured can be divided into two separate parts, one of them constant and the other a fractional error. Each of them depends on the power supply used to create the potential in the CVC. This can be modeled using the equation:

$$\Delta I = \sqrt{(N_I - 1)}\,(e_{constant} + e_{fractional} \bullet V_{applied}) \qquad [3]$$

N_I = Sampling Rate
$e_{constant}$ = constant error
$e_{fractional}$ = fractional error

Previous Methods

Previously the method for measuring conductivity of highly disordered insulating materials involved the use of a standard high voltage Bertan power supply for low voltages, with a short time scale noise dominated by the ±250 mV AC ripple and long time scale fluctuations driven by diurnal temperature-driven instabilities in the control voltage amplifier (8). In Analyzing the Bertan power supply and the battery power supply we were able to find values for both the fractional and constant error for both (Table 1).

This ripple is significant as it propagates through all of the measurements of the conductivity curve, and can seriously skew results. Even in the idealized charge propagation model, it is easy to see how this ripple can have an effect on the current that is measured on the back side (Fig. (4)). In the realistic charge propagation it is easy to see how uncertainty in the measurements of the gradual change in current would be

dominated by this ripple. This effect increases the error associated with our current measurements thus decreasing the certainty involved with conductivity measurements.

Previous experiments were performed to determine a method to decrease this ripple, and a constant voltage battery power supply was determined to decrease the noise by an order of magnitude (8). For this reason, a high voltage battery power supply was created and used to measure currents supplied by voltages as high as 1000 V.

Modifications

To demonstrate a decrease in noise associated with conductivity measurements, a high voltage battery supply was designed and built consisting of three hundred thirty three 3 V. watch batteries aligned in series. Grouping the batteries in 500, 250, 100, 50… 3 V independent packages allowed selection of any voltage from 3 V to 1000 V in 3 V increments. See Figure (5).

A detailed electrical schematic has been generated (see Appendix A) to more easily identify grounding loops, inadequate shielding, and noise issues associated with improper use of the filtered A/C power strip. This schematic has also helped to better understand the subtle details of how grounds are handled in the data acquisition interface box (NI BNC-2110) allowing for more accurate and responsive data acquisition (8).

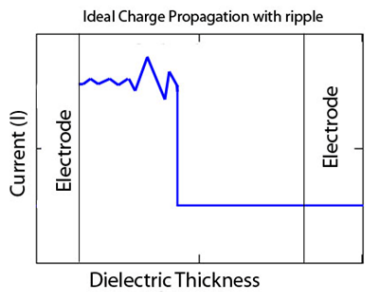

Figure (4) an illustration of what the ideal charge propagating wave would look like with uncertainty involved.

As the battery power supply was built a schematic was written and through the use of this drawing, potential issues with the battery power supply were identified, isolated and solved. One example of this was a need to create low voltage potentials while conserving the number of ports possible on the power supply. A drawing allowed us to produce an ingenious method involving points of contact positioned between batteries aligned in series.

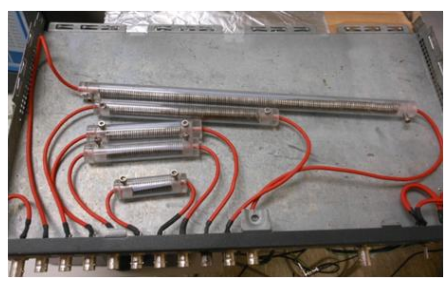

Figure (5) picture of the finished Battery power supply.

This schematic was then combined with the schematic for the whole CVC chamber which contains all of the mechanical systems including the vacuum and cryogenic layouts. This allowed for a more complete picture of the system as a whole. This is vital to locating and correcting leaks

Table 1 Values for various errors associated with the Bertan power supply, and a battery power supply.

Source	High Voltage Bertan Power Supply	High Voltage Battery Supply
Constant error	250 mV	16 mV
Fractional error	0.001*voltage	16 ppm*voltage
Voltage error	±0.3 V	±0.02 V

in the liquid nitrogen system, finding where to connect electrodes within the chamber, and locating lost grounds. Resolving these issues has allowed more precise measurements over temperatures ranging from 100 K to 350 K and voltages from 3 V to 1000 V.

Data Analysis

Analyzing data taken with the CVC has been challenging due, in large part, to the immense amount of data acquired with this system. Data runs typically span many orders of magnitude in time (up to 10^5 s duration at 1 ms to 10 s intervals) making them difficult to repeat if a problem occurs during a run. A method of data analysis has been developed which uses multiple programs (Labview, Excel, and IGOR pro) to rapidly analyze data, and evaluate the system's performance. These programs use an adaptive binning algorithm to calculate mean averages for the current measurements. From this, the statistical error is applied to the data spread using Eq. [2] for each n_{pnts} bin:

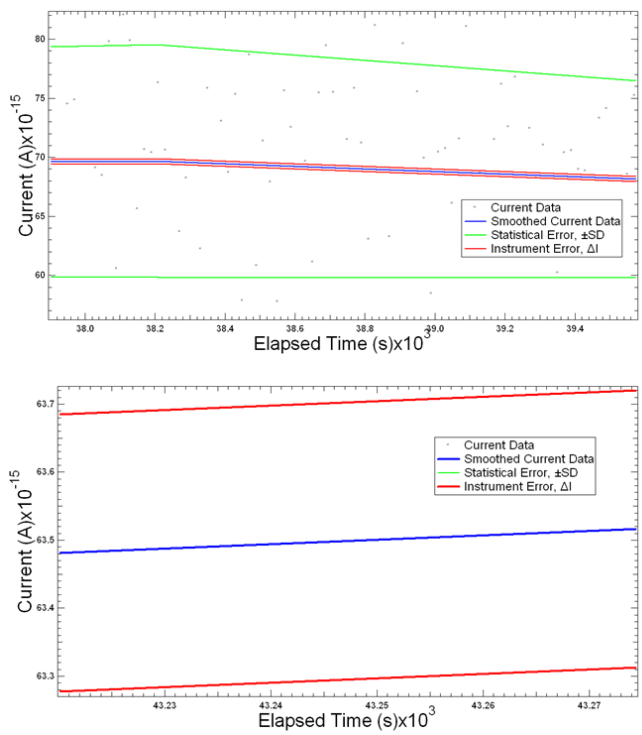

Chart 1 Graphs of current data taken using Bertan power supply. (a) Variation in statistical error. (b) Variation in instrument error.

$$\Delta\sigma_{SD} = \sqrt{\frac{1}{npnts-1}\sum(Y_i - npnts_avg)^2} \qquad [4]$$

An instrumentation error document (9) has been generated outlining the error associated with each piece of equipment used in the CVC. This document incorporates second order error calculations based on quantities such as the response time of the low level electrometer and operating frequency of the data acquisition card; constant and relative error of the applied voltage associated with the power supply and current measured with the electrometer, as well errors in sample and electrode measurements. The voltage error Eq. [3], current error Eq. [4], and instrument error Eq. [5] are calculated for each bin and applied to the corresponding graphs (see CVC Error Analysis v1_7 document for a detailed explanation of these equations).

$$\Delta V = (N_V - 1)^{-\frac{1}{2}} \cdot [250\ mV + 0.1\% \cdot V] \qquad [5]$$

$$\Delta I_{err}(I,R,S) = \left[N_{bin}\cdot(N_I-1)\cdot\min\left(1,\frac{100}{T_R(R)\cdot f_I}\right)\right]^{-\frac{1}{2}}\cdot\left[|I|\cdot\left(\Delta F_{elec}(R)+\Delta F_{DAQ}\right)+(10^R\cdot A)\cdot\left[\Delta I_R\cdot\right.\right.$$

$$1.4-0.4\cdot 3-S+\Delta ID\cdot 10S-2 \quad [6]$$

$$\Delta\sigma = \sigma\cdot\sqrt{\left(\frac{\Delta I_{err}}{I}\right)^2+\left(\frac{\Delta V}{V}\right)^2} \quad [7]$$

- N_V = Number of samples taken for a given voltage data set,
- V = Measured voltage,
- I = Current measured by the electrometer,
- R = Electrometer current range setting,
- S = Electrometer display sensitivity setting,
- ΔF_{elec} = Electrometer range resolution factor at a given range, *R,*
- T_R = Rise time (response time of the meter for a current change from 10% to 90% of full scale) at a given range, *R* ,
- ΔF_{DAQ} = DAQ resolution factor,
- N_I = Number of samples taken for a given current data set,
- f_I = Sampling rate of DAQ card,
- ΔI_R = Range resolution,
- ΔI_D = DAC card error for least significant bit (LSB).

By comparing the statistical error, $\Delta\sigma_{SD}$, to the instrument error, $\Delta\sigma$, a quantitative assessment of how well the chamber is performing can be made (8).

Results

Three data sets have been chosen for comparison of instrumentation performance and quality of data. All measured samples are $27.4 \pm 0.5\%\ \mu m$ thick Low Density Polyethylene (LDPE) with an applied electric potential of 100 V or 500 V. The first data run, (LDPE 27.4 100V RT filter test 3-26-2009) was taken with the use of the Bertan power supply (see Chart 1). The second and third data runs (LDPE 100 V 12 hr battery test 2-21-201; and LDPE 500 V 96 hr battery 4-13-2014) were taken with the modified battery power supply (see Charts 2 and 3, respectively). The reason for using two 100 V runs is to show a decrease in uncertainty. The 500 V run will be used to demonstrate that a voltage increase does not affect the amount of uncertainty associated with the measurements.

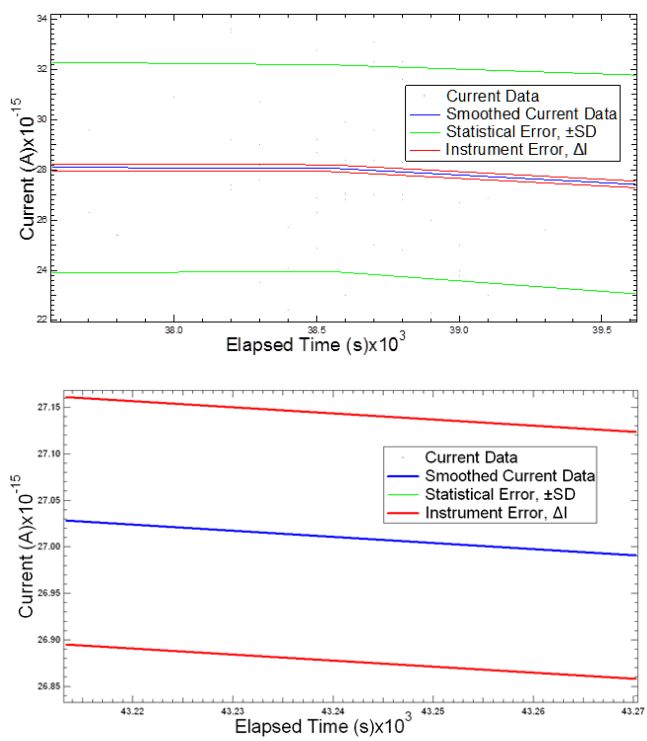

Chart 2 Graphs of current data taken using battery power supply at 100 V. (a) Variation in statistical error (b) Variation in instrument error

The test run taken on 3-26-2009 was a run measuring the conductivity of a sample of LDPE which had a potential of 100 V applied to it. For the run, the electric potential was applied for $3.4 \cdot 10^{5}$ s (4 days), until the current had reached equilibrium. The voltage was then turned off, and the sample was allowed to discharge. The discharge was not the focus of this study, and so it was left off from the analysis. Analysis of the measurements found that the statistical error was $\pm 1 \cdot 10^{-14}$A. (Chart 1(a)) Analysis of the instrumental error was also performed and that was found to be $\pm 2 \cdot 10^{-16}$ A (Chart 1(b))

The test run taken on 2-21-14 was a similar run to the first run. The conditions surrounding this test were all identical to those on the first test, except for the voltage supply used, and the length of the test. The length of the test however is irrelevant to the tests when comparing the error associated with the individual data points. After careful analysis of these data, it was found that the statistical error was $\pm 410^{-15}$ A, only 40% of the error of the initial run (see Chart 2(a)). The instrument error had a value of $\pm 1.4 \cdot 10^{-16}$ A (see Chart 2(b)).

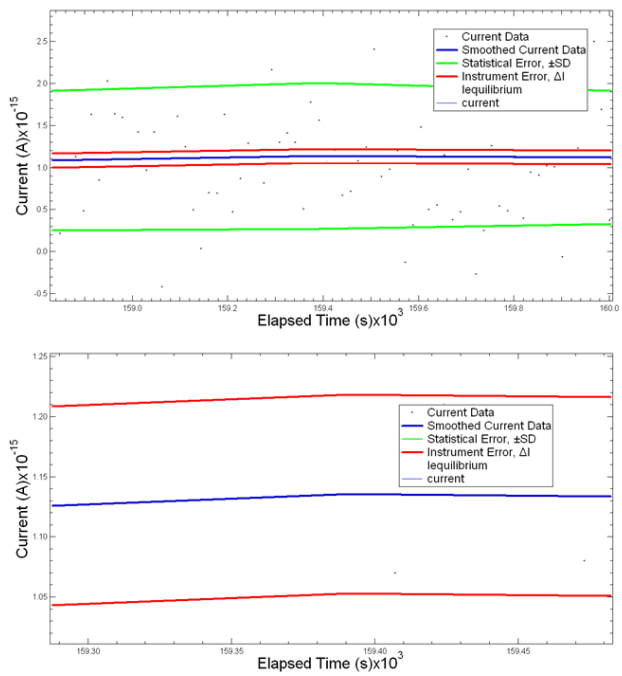

Chart 3 Graphs of current data taken using battery power supply at 500 V. (a) Variation in statistical error. (b) Variation in instrument error.

The run made on 4-13-2004 was performed to insure that the error associated with the battery at higher voltages remained fairly consistent. The statistical error was $\pm 9 \cdot 10^{-17}$ (see Chart 3(a)) and the instrument error was $\pm 8 \cdot 10^{-17}$ Chart 3(b) The CVC is programmed to take 100 measurements per second. With an error as low as 10^{-17}, the CVC is effectively measuring about 6 electrons each time it takes a data point.

After plotting the data from 4-13-2004 in a chart of current vs. time, it was easy to see the exponential decrease that was exhibited by the current. In an effort to determine when each of the different individual portions of the overall current (polarization, diffusion, dispersion, and saturation) were dominant, Log current was plotted against time. (Chart 4(a)). From this plot, we see that the instrument rise time and polarization current are exponentials solely dependent upon time, but the graph still has an nonlinear decrease. This nonlinear decrease leads us to believe that there is a different portion of the current which becomes dominant at the point on the graph where the slope changes. A plot of log current vs. log time was created (Chart 4(b)). On this graph the slopes for the instrument rise time, polarization current, diffusion current, dispersion current, and equilibrium current were found by plotting slopes for the individual straight lines.

An anomaly did occur when the data were plotted in this log vs. log graph. Notice the straight line which has a different slope beginning time $t=10^{2}$ s and ending at roughly 10^{3} s that seems to be cut through by

the polarization current. This appears to have been caused by either, the proximity of a human to the machine, (10) or human error in turning knobs prematurely while acquiring data.

Through this data analysis a very nice model has been formed which shows the magnitude of the rates for the different portions of current flowing thorough highly resistive materials. Thus a model has been formed to show all of the different portions of current in a conductivity curve, (Equation 8):

$$I(t) = (1 - e^{\frac{t}{0.2s}}) + I_{polarization} e^{\frac{t}{\tau_{pol}}} + I_{diffusion} t^{-\tau_{diff}} + I_{Dispersion} t^{-\tau_{disp}} + I_{equilibrium} \qquad [8]$$

$$I_{polarization} = e^{-5.707t \times 10^{-15}} \qquad \tau_{polarization} \approx 15s$$

$$I_{dispersion} = e^{-2t \times 10^{-18}} \qquad \tau_{dispersion} = 3000s$$

$$I_{diffusion} = e^{-5.227t \times 10^{16}} \qquad \tau_{diffusion} \approx 1000s$$

$$I_{Equilibrium} = 1.6022 \times 10^{-15} A$$

Future work

Continued development of the CVC chamber would involve continuing to test materials within the temperature limits of the instrument, and continued development of the CVC analysis program expanding its capabilities. A major contributor to the precision of the CVC can be attributed to the use a higher voltage battery power source. Unfortunately, a battery power source is not practical for achieving voltages in excess of 2000 V, high enough for long time duration discharge calculations. The use of the high (1000-10,000 V) voltage power supply will still need to be employed. One method to decrease the error associated with this power supply would be to use a series of capacitors constantly charging and discharging to achieve a more stable constant voltage. Some testing has been done with a capacitor driven power source, with no apparent success, however, scientists in Japan have performed CVC experiments using capacitor driven power supplies to provide very high voltages (1000-10,000 V) while maintaining uncertainty comparable to that relating to a battery power supply.

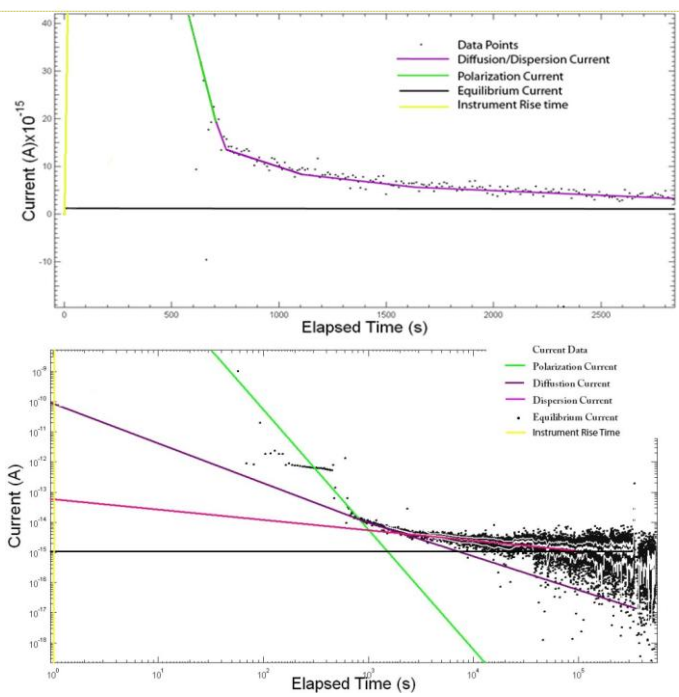

Chart 4. (a) Chart showing log current vs. time (s). (b) Chart showing log current vs. log time with all of the different portions of current plotted as well.

Formatted: Font: 12 pt

Continued temperature dependant testing should be carried out, since a procedure for cooling and heating the chamber during the same run has been developed. Liquid nitrogen cooling should yield good results now that many of the main electrical vacuum feedthrough gaskets have been replaced. Once the chamber has reached room temperature, the heating elements may be used to raise the temperature up to 80 C. (Beyond this the integrity of parts in the chamber may become compromised.)

Improvements to the CVC analysis program will be an ongoing process. Plot adjustments and fine tuning may be done as new information about the system is needed. The program is documented (in red) very well so generating an understanding of how it works is possible. IGOR has many curve fitting options making it a useful tool for further analysis and model testing. Preliminary curve fitting has been applied to test runs taken on 3-26-2009 and 2-6-2009 using the abbreviated time dependant conductivity model (9) shown in Eq. [9]:

$$\sigma_{model}(t) = \sigma_{pol} \cdot e^{\left(-\frac{t}{\tau_{pol}}\right)} + \sigma_{SC} \cdot t^{(-\alpha)} + \sigma_{DC} \qquad [9]$$

where the instument rise time term is omited, the $\sigma_{pol} \cdot e^{\left(-\frac{t}{\tau_{pol}}\right)}$ term represents the polarization effects, the $\sigma_{SC} \cdot t^{(-\alpha)}$ term represents the diffusive/dispersive behavior related to space charge, and the σ_{DC} term is the constant long timescale equilibrium dark current. Note the polarization term is attempting to fit data points not seen in this scale (an artifact of the binning algorithm used for smoothing, which has a minimum of 6 data points for any bin), hence the deviation for the initial part of the curves.

Conclusion

The introduction of a high-voltage battery power supply has reduced the error associated with conductivity measurements taken in the CVC chamber for highly disordered insulating materials. The uncertainty involved with measurements of statistical error has been decreased by an order of magnitude, and the uncertainty associated with instrument error has been decreased by half. Through measurements of various voltages it has been determined that this decrease in uncertainty is independent of the voltage applied to the sample. Because of an improved power supply we can successfully measure, with a large degree of certainty, currents as low as tens of atto-amps.

Through careful measurements a model has been created showing that a conductivity curve can be broken down into five individual component currents. The slopes for each of these currents were measured, and through the use of curve fitting, plotted against a model. This model agrees well with literature for conductivity calculations of LDPE. Conductivity values obtained with the CVC show good promise for reliable knowledge of decay times for LDPE which is used extensively in the construction of modern spacecraft, insulation of terrestrial transmission lines, and may be used in the future as a more efficient power container in capacitor driven power supplies. The improvements made to the chamber will prove beneficial to future measurements taken with the system although more can be done to reach the instruments theoretical limit.

References

(1) How Much Electricity Is Lost in Transmission and Distribution in the United States? Rep. N.p.: n.p., n.d. Web. 22 Apr. 2014. <http://www.eia.gov/tools/faqs/faq.cfm?id=105&t=3>.

(2) Hoffmann, R., J. Dennison, et al. (2008). "Low-Fluence Electron Yields of Highly Insulating Materials." IEEE Transactions on Plasma Science 36(5 Part 2): 2238-2245.

(3) D. Hastings, H. Garrett, Spacecraft-Environment Interactions, New York, NY: Cambridge Press, 1996.

(4) Brunson, Jerilyn, "Hopping Conductivity and Charge Transport in Low Density Polyethylene" (2010). PhD Dissertation, Utah State University, Logan, UT.

(5) Adamec, V. and J. Calderwood (1981). "On the determination of electrical conductivity in polyethylene." Journal of Physics D: Applied Physics 14(8): 1487-1494.

(6) Phil Lundgreen, JR Dennison and Justin Dekany, "Methods to Decrease Error in Conductivity Measurements of Highly Disordered Insulating Materials," Utah Conference for Undergraduate Research, Brigham Young University, Provo, UT, Feb 28, 2014.

(7) Justin Dekany, JR Dennison and Alec Sim, "Reduction and Characterization of Error in Low Current Measurements," American Physical Society Four Corner Section Meeting, Colorado School of Mines, Golden, CO, October 23-24, 2009.

(8) Justin Dekany, JR Dennison and Alec Sim, "Evaluation of Constant Voltage Chamber Modifications," Phys 4900 paper, Utah State University, Logan, UT, April 20, 2010.

(9) J.R. Dennison, Jerilyn Brunson, Alec Sim, Justin Dekany, Ryan Hoffman, Steve Hart, Joshua Hodges and Amberly Evans, USU Materials Physics Group internal document (CVC Error Analysis), Logan, UT, 2009.

(10) Joshua Hodges (2013), "In Situ Measurements of Electron-Beam-Induced Surface Voltage of Highly Resistive Materials," Masters Thesis, Utah State University, Logan, UT.
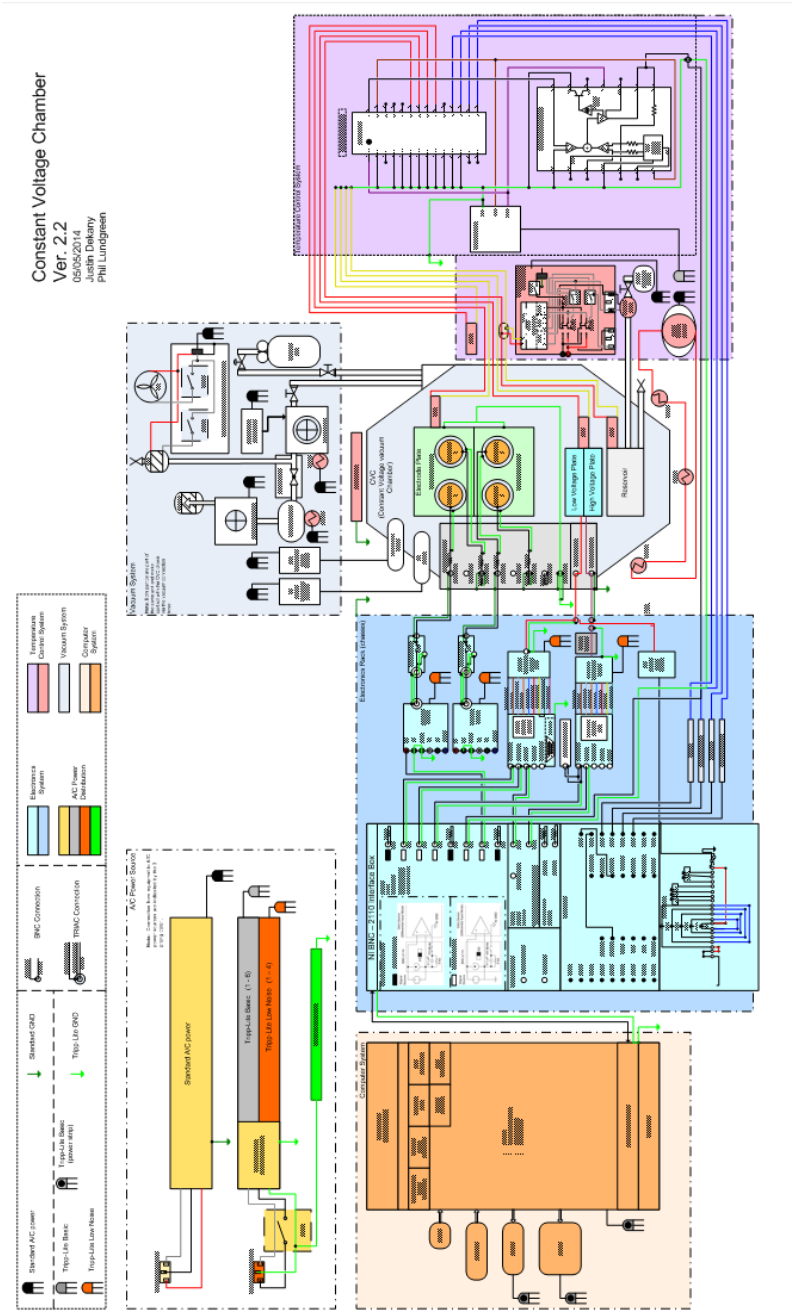
Appendix A – Constant Voltage Chamber Schematic